
Article:
Ran, Q., Tong, J., Shao, S. et al. (2 more authors) (2015) Incompressible SPH scour model for movable bed dam break flows. Advances in Water Resources, 82. 39 - 50. ISSN 0309-1708

https://doi.org/10.1016/j.advwatres.2015.04.009

Incompressible SPH Scour Model for Movable Bed Dam Break Flows

Qihua Ran
Professor, Department of Hydraulic Engineering, Zhejiang University, Hangzhou 310058, China.
Email: ranqihua@zju.edu.cn

Jian Tong
Postgraduate student, Department of Hydraulic Engineering, Zhejiang University, Hangzhou 310058, China.
Email: tstj9022@zju.edu.cn

Songdong Shao
Senior Lecturer, Department of Civil and Structural Engineering, University of Sheffield, Sheffield S1 3JD, United Kingdom. (Visiting Professor, State Key Laboratory of Hydro-Science and Engineering, Tsinghua University, Beijing 100084, China)
E-mail: s.shao@sheffield.ac.uk (Author of Correspondence)

Xudong Fu
Professor, State Key Laboratory of Hydro-Science and Engineering, Tsinghua University, Beijing 100084, China
Email: xdfu@tsinghua.edu.cn

Yueping Xu
Professor, Department of Hydraulic Engineering, Zhejiang University, Hangzhou 310058, China.
Email: yuepingxu@zju.edu.cn

Abstract

In this study an incompressible Smoothed Particle Hydrodynamics (ISPH) approach coupled with the sediment erosion model is developed to investigate the sediment bed scour and grain movement under the dam break flows. Two-phase formulations are used in the ISPH numerical algorithms to examine the free surface and bed evolution profiles, in which the entrained sediments are treated as a different fluid component as compared with the water. The sediment bed erosion model is based on the concept of pick-up flow velocity and the sediment is initiated when the local flow velocity exceeds a critical value. Also, a simple viscosity model is used to correct the fluid viscosity due to the mixing of the sediment materials with water. The proposed model is used to reproduce the sediment erosion and follow-on entrainment process under an instantaneous dam break flow and the results are compared with those from the weakly compressible Moving Particle Semi-implicit (WCMPS) method as well as the experimental data. It has been demonstrated that the two-phase ISPH model performed well with the experimental data. The study shows that the ISPH modelling approach can accurately predict the dynamic sediment scouring process without the need to use empirical sediment transport formulas.

Keywords:

ISPH, dam break, movable bed, pick-up velocity, scour model, two-phase

Introduction

Dam break flows can release a huge amount of water in a short period of time and drastically change the local topographies, leading to serious flooding waves and sediment transports. Dam break flows over a fixed impermeable bed have been extensively studied, but such flows over a movable layer of materials need more investigations. The general flow situations and underlying hydrodynamics under fixed and movable bed conditions are significantly different and they heavily influence the free surface deformations and flooding wave propagations. Therefore, it is of great theoretical and practical interest to study these kinds of the flow (Lauber and Hager, 1998; Janosi et al., 2004).

Numerical studies and modelling techniques have been widely used as a robust tool to investigate a variety of dam break flows over the movable bed with sediment erosion and deposition process. For example, Zhang and Duan (2011) used the 1D Shallow Water Equations (SWEs) and Exner equation to study flood routing over a mobile alluvium based on the Finite Volume (FV) approach. Xia et al. (2010) used the modified 2D SWEs coupled with a graded sediment transport equation to study mobile bed evolutions and an unstructured Finite Volume algorithm was used to solve the governing equations. These above numerical methods can be classified as the grid modelling technique, i.e. a computational grid is used in the computational domain. However, the common feature of grid modelling techniques is that the hydrodynamic equations are solved based on fixed grid system and this could cause the problem of numerical diffusion due to the advection term in the equations, especially when the free surface is under large deformation such as found in the dam break flow conditions.

In contrast, the mesh-free particle methods use each individual particle to track the flow motion, so they are capable of simulating many kinds of the free surface flow with large free boundary and interface deformation and fragmentation. These methods have also been efficiently used to the dam break flows over erodible bed. For example, Hayashi et al. (2003) used the Moving Particle Semi-implicit (MPS) method combined with a bed scour model based on erosion velocity to compute the seawall toe scouring due to a dropping jet. Shakibaeinia and Jin (2011) used the weakly compressible MPS formulation together with different rheological models to compute an unsteady dam break flow over movable bed. On the other hand, the Smoothed Particle Hydrodynamics (SPH) method has recently been explored in many coastal and hydraulic applications due to its high accuracy and flexibility in adapting to a wide range of flow scenarios. SPH directly discretises the fluid medium using the fluid particles rather than fixed grids. So it can naturally support the simulations of dynamic interaction among the multiple fluid media as well as any large relative motions. As for the SPH application in movable bed dam break flows, although underreported, Sibilla (2008) used the SPH to compute water phase and Exner equation to compute sediment phase of bed evolution by using a standard finite-difference scheme, and the model was used to predict the scouring process under a sluice gate with satisfactory results. A follow-on work of Manenti et al. (2012) included the soil yielding criterion and sediment Shields theory to investigate non-cohesive sediment movement in an artificial reservoir. In the latest large scale

SPH applications in complex marine-engineering field, Ulrich et al. (2013) proposed an effective water-soil suspension model to reproduce the Louvain dam break erosion experiment.

The study in this paper aims to use the incompressible SPH (ISPH) concept (Cummins and Rudman, 1999; Shao and Lo, 2003) as the fundamental numerical tool to study the dam break flows and subsequent erosions and entrainments of the sediment grain. The ISPH uses a truly hydrodynamic formulation to compute the fluid pressure and thus it can obtain a relatively more stable velocity and pressure field. This is important to provide accurate flow information to the coupled sediment erosion model, since the sediment phase calculation is very sensitive to the particle fluctuation and pressure noise. In view of the existing SPH practice to model the mobile bed scouring, they generally fall into two distinct categories. One is to treat the water and sediment media as two different fluid components and an interaction model is used to address the discontinuity of the two phases (Shakibaeinia and Jin, 2011), while another is to consider the critical velocity and shear stress of the flow acting on the sediment bed and treat the bed as an erodible solid wall (Hayashi et al., 2003). The latter approach is explored in present paper as we think it could more realistically reflect the sediment erosion and scouring mechanism, which is consistent with the empirical sediment principles adopted by the engineering practice. The sediment erosion model is based on the formulations of Ikari et al. (2010), in which a straightforward and effective pick-up flow velocity concept was used to initiate the sediment motion, and sea cliff erosions from the continuous wave attacks were well predicted.

This paper is structured as follows. First the principles of ISPH method and two-phase modelling concept of the water-sediment mixture are presented, followed by the sediment erosion model. Then the relevant numerical boundary conditions are briefly described. In the model applications, two benchmark laboratory experiments of dam break flow over a movable bed made of sediment materials are investigated. The computed results of the free surface and sediment scour profiles are validated by the documented experimental and numerical data. Besides, additional numerical tests are carried out to study the influence of particle resolution and threshold pick-up velocity on the flow and sediment movement features and two-phase velocity and pressure fields are analyzed near the water-sediment interface to demonstrate the scouring mechanisms.

Principles of Two-Phase ISPH Model

Governing Equations

In the single-phase ISPH algorithm, the 2D hydrodynamic equations are represented in the following Lagrangian form as:

$$\frac{1}{\rho}\frac{\mathrm{d}\rho}{\mathrm{dt}} + \nabla \cdot \mathbf{u} = 0 \tag{1}$$

$$\frac{\mathrm{d}\mathbf{u}}{\mathrm{dt}} = -\frac{1}{\rho}\nabla \mathrm{P} + \mathbf{g} + \nu_0 \nabla^2 \mathbf{u} + \frac{1}{\rho}\nabla \cdot \vec{\boldsymbol{\tau}} \tag{2}$$

where ρ = density; t = time; $\mathbf{u}$ = velocity vector; P = pressure; $\mathbf{g}$ = gravitational acceleration vector; ν_0 = kinematic viscosity; and $\vec{\boldsymbol{\tau}}$ = sub-particle scale (SPS) turbulent stress.

The turbulent stress $\vec{\boldsymbol{\tau}}$ in Equation (2) should be considered in the dam break flows, as the computational particle scale is much larger than the flow turbulent structure. By following an eddy viscosity formulation, which was originally proposed by Gotoh et al. (2001) for the turbulent jet, we have

$$\tau_{\mathrm{ij}} / \rho = 2\nu_{\mathrm{T}} \mathrm{S}_{\mathrm{ij}} - \frac{2}{3}\mathrm{k}\delta_{\mathrm{ij}} \tag{3}$$

where ν_{T} = turbulent eddy viscosity; S_{ij} = strain rate of the mean flow; k = turbulent kinetic energy; and δ_{ij} = Kronecker's delta. Here the Smagorinsky model is used to compute the turbulent eddy viscosity ν_{T} as follows:

$$\nu_{\mathrm{T}} = (\mathrm{C_s}\Delta \mathrm{X})^2 \left|\mathrm{S}\right| \tag{4}$$

where $\mathrm{C_s}$ = Smagorinsky constant, which is taken as 0.12 in the paper; ΔX = particle spacing, indicating the characteristic length scale of the small eddies; and $\left|\mathrm{S}\right| = (2\mathrm{S_{ij}}\,\mathrm{S_{ij}})^{1/2}$ is the local strain rate.

Two-step Solution Procedure

The ISPH model uses a two-step projection approach similar to Cummins and Rudman (1999) to solve Equations (1) and (2). The first step is fully explicit, to predict an intermediate particle velocity and position without using the pressure term

$$\Delta \mathbf{u}_* = (\mathbf{g} + \nu_0 \nabla^2 \mathbf{u} + \frac{1}{\rho}\nabla \cdot \vec{\boldsymbol{\tau}})\Delta \mathrm{t} \tag{5}$$

$$\mathbf{u}_* = \mathbf{u}_{\mathrm{t}} + \Delta \mathbf{u}_* \tag{6}$$

$$\mathbf{r}_* = \mathbf{r}_{\mathrm{t}} + \mathbf{u}_* \Delta \mathrm{t} \tag{7}$$

where $\Delta\mathbf{u}_*$ = increment of particle velocity in the prediction step; Δt = time increment; $\mathbf{u}_t$ and $\mathbf{r}_t$ = particle velocity and position at time t; and $\mathbf{u}_*$ and $\mathbf{r}_*$ = intermediate particle velocity and position.

The second step is implicit, to correct the particle velocity by using the pressure as:

$$\Delta\mathbf{u}_{**} = -\frac{1}{\rho_*}\nabla P_{t+1}\Delta t \tag{8}$$

$$\mathbf{u}_{t+1} = \mathbf{u}_* + \Delta\mathbf{u}_{**} \tag{9}$$

where $\Delta\mathbf{u}_{**}$ = increment of particle velocity in the correction step; ρ_* = intermediate particle density calculated after the prediction step; and P_{t+1} and $\mathbf{u}_{t+1}$ = particle pressure and velocity at time $t+1$.

The finally updated particle positions are computed by using a central difference scheme in time as:

$$\mathbf{r}_{t+1} = \mathbf{r}_t + \frac{(\mathbf{u}_t + \mathbf{u}_{t+1})}{2}\Delta t \tag{10}$$

where $\mathbf{r}_t$ and $\mathbf{r}_{t+1}$ = positions of the particle at time t and $t+1$, respectively.

The pressure of the fluid particle is calculated from the pressure Poisson equation (PPE) as

$$\nabla\cdot\left(\frac{1}{\rho_*}\nabla P_{t+1}\right) = \frac{\rho_0 - \rho_*}{\rho_0 \Delta t^2} \tag{11}$$

where ρ_0 = initial constant density of the particle.

Here it should be noted that the above two-step solution procedure based on PPE Equation (11) is solved to guarantee the density invariance. This formulation has also been investigated by other authors such as Hu and Adams (2007), Xu et al. (2009) and Lind et al. (2012), who have concluded that this formulation is not very accurate and thus different corrections were proposed. In this study, we did not include these modifications as the simulation time is relatively short for the dam break flow and the above-raised accuracy issues were not experienced.

SPH Theory and Formulations

The SPH formulations as developed by Monaghan (1992) are obtained by interpolating from a set of points that are disordered. The interpolation is based on the theory of integral interpolants using kernels to approximate a delta function. The interpolants are the analytic

functions that can be differentiated without the use of a grid. The SPH equations describe the motion of the interpolating points, which can be thought of as the particles.

In summary, the density ρ_a of a particle a is calculated by

$$\rho_a = \sum_b m_b W(|\mathbf{r}_a - \mathbf{r}_b|, h) \tag{12}$$

where a and b = reference particle and its neighbours; m_b = particle mass; $\mathbf{r}_a$ and $\mathbf{r}_b$ = particle position vectors; W = interpolation kernel; and h = smoothing distance, which limits the range of particle interactions and is taken as 1.2 times of the initial particle spacing ΔX in this paper. There are several types of the kernel available in the literatures (cubic, quintic, etc). Here we use the spline kernel normalized in 2D (Monaghan, 1992) after balancing the computational accuracy and efficiency. This kernel has the advantages of compact support, continuous second derivative, and is globally second-order accurate. The gradient of the particle pressure is calculated as

$$(\frac{1}{\rho}\nabla P)_a = \sum_b m_b (\frac{P_a}{\rho_a^2} + \frac{P_b}{\rho_b^2}) \nabla_a W_{ab} \tag{13}$$

where the summation is over all the particles other than particle a; and $\nabla_a W_{ab}$ = gradient of the kernel taken with respect to the position of particle a. The turbulent stress in Equation (2) is formulated by applying the SPH definition of divergence as

$$(\frac{1}{\rho}\nabla \cdot \vec{\boldsymbol{\tau}})_a = \sum_b m_b (\frac{\vec{\boldsymbol{\tau}}_a}{\rho_a^2} + \frac{\vec{\boldsymbol{\tau}}_b}{\rho_b^2}) \cdot \nabla_a W_{ab} \tag{14}$$

Due to the high sensitivity of fluid pressure arising from the particle disorder, the Laplacian in the PPE equation (11) is formulated through a hybrid of the standard SPH first derivative with a first-order finite difference scheme (Shao and Lo, 2003), and the same rule is also applied to model the viscosity term in Equation (2) as follows

$$\nabla \cdot (\frac{1}{\rho}\nabla P)_a = \sum_b m_b \frac{8}{(\rho_a + \rho_b)^2} \frac{(P_a - P_b)(\mathbf{r}_a - \mathbf{r}_b) \cdot \nabla_a W_{ab}}{|\mathbf{r}_a - \mathbf{r}_b|^2} \tag{15}$$

and

$$(\nu_0 \nabla^2 \mathbf{u})_a = \sum_b m_b \frac{2(\nu_a + \nu_b)}{\rho_a + \rho_b} \frac{(\mathbf{u}_a - \mathbf{u}_b)(\mathbf{r}_a - \mathbf{r}_b) \cdot \nabla_a W_{ab}}{|\mathbf{r}_a - \mathbf{r}_b|^2} \tag{16}$$

Concept of Two-Phase ISPH Approach

After a boundary particle is initiated from the bed scouring, it can change its identification in two different ways, i.e. as a pure water particle or as a sediment particle. If

the sediment concentration is low, or the density of the sediment grain is close to that of the water, we can simply treat the water-sediment mixture as a single phase. That is to say, the standard ISPH solution algorithms as presented above are applicable. However, if the existence of the sediment particles has generated an obvious impact on the flow property, a two-phase modelling technique should be considered in the numerical scheme. Here we follow the multi-fluid ISPH formulation of Shao (2012) to model the water-sediment mixtures after the sediment grain is eroded from the bed and mixed with the dam break water. The general principles are reviewed as below.

The two-phase ISPH model is based on the general multi-phase flow equations, and the mass and momentum equations are represented by

$$\frac{1}{\rho_{\mathrm{m}}}\frac{\mathrm{d}\rho_{\mathrm{m}}}{\mathrm{dt}}+\nabla\cdot\mathbf{u}_{\mathrm{m}}=0 \tag{17}$$

$$\rho_{\mathrm{m}}\frac{\mathrm{d}\mathbf{u}_{\mathrm{m}}}{\mathrm{dt}}=-\nabla\mathrm{P}_{\mathrm{m}}+\rho_{\mathrm{m}}\mathbf{g}+\mu_{\mathrm{m}}\nabla^{2}\mathbf{u}_{\mathrm{l}}+\nabla\cdot\vec{\boldsymbol{\tau}}+\mathbf{f}_{\mathrm{m}} \tag{18}$$

where $\mathrm{m}=\mathrm{l},\mathrm{s}$ refers to the liquid and solid phases, respectively; and $\mathbf{f}_{\mathrm{m}}$ = unknown interaction force between the two different phases, which makes it different from the single-phase equations (1) and (2).

The solution method of the two-phase ISPH is generally similar to that of the single-phase ISPH in both the prediction and correction steps. However, to obtain the appropriate pressure field to correct the particle parameters across the two-phase interface, Gotoh and Sakai (2006) combined the continuity and momentum equations and derived a unified pressure Poisson equation that includes the interaction of two different phases as:

$$\nabla\cdot(\frac{1}{\rho_{\mathrm{m}}}\nabla\mathrm{P})=\frac{\rho_{0}-\rho_{*}}{\rho_{0}(\Delta\mathrm{t})^{2}} \tag{19}$$

As a result, in the correction step we apply the pressure computed from the above equation to both the water and sediment particles to correct their velocities and update their spatial locations. In the coupled two-phase ISPH algorithm (Shao, 2012), it has been assumed that the search of neighbouring particles includes the different phases. This implied that the unknown interaction force $\mathbf{f}_{\mathrm{m}}$ in Equation (18) can be dropped if the pressure is solved by Equation (19).

To further improve the two-phase modelling performance, the effective viscosity of the sediment-laden flow should also be corrected to reflect the existence of sediment suspension. The simplest approach would be to use a Newtonian formulation suggested by Shakibaeinia and Jin (2011) using the following relationship

$$\mu_{\mathrm{mixture}}=\mu_{\mathrm{liquid}}/(1+\mathrm{C}\frac{\rho_{\mathrm{s}}}{\rho_{\mathrm{l}}})^{1/2} \tag{20}$$

where C = volumetric fraction of the sediment phase. In the computation this is evaluated by searching the neighbours of the reference sediment particle and then counting the percentage of the sediment grain. As pointed out by Shakibaeinia and Jin (2011), this simple Newtonian relation may not be able to correctly reflect the behaviour of granular flows and thus they further suggested non-Newtonian properties of the fluid be considered.

ISPH Erosion Model

To compute the scouring process of a movable bed by the ISPH model, we define five different types of the particles, i.e. dummy particle, impenetrable wall particle, inner water particle, interface contact particle and scoured particle, as shown in Fig. 1. Among them, the dummy particles are used outside of the solid wall boundary to keep the density of the wall consistent with that of the inner fluid to prevent flow penetration. The interface contact particles are the special wall particles located on the water-sediment bed interface, which can be eroded and converted into the inner water particles. If the threshold erosion criterion is met (which will be explained later), the interface contact particles are initiated and entrained into the main flow. Then they are flagged as the inner water (or sediment) particles and meanwhile, a new layer of the interface contact particles are generated from the nearest dummy particles. Furthermore, another new layer of the dummy particles are also automatically generated to maintain the kernel compactness near the solid wall. In the ISPH computations, this erosion/scouring process can continue until the flow velocity balances the sediment resistance capacity so that no further erosion/scouring happen. As can be seen, the dummy particles serve as two different purposes, i.e. to balance the pressure of the inner fluid particles and to supplement the potential interface contact particles.

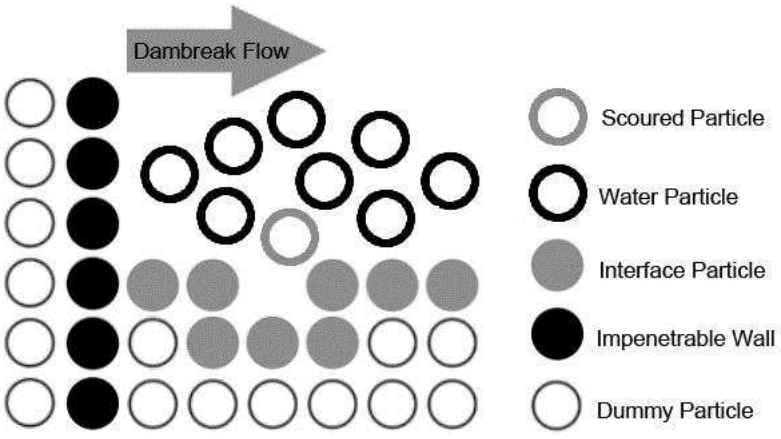

Fig. 1 Different types of particles near movable bed in ISPH erosion model

To judge the initiation of movable bed particle under the threshold condition, a so-called "pick-up" velocity concept is used, in which the initiation of a bed wall particle depends on the flow situation represented by its neighbouring inner water particles. By following Hayashi et al. (2003) and Ikari et al. (2010), both the normal and the tangential velocity components of the flow are used to evaluate the sediment initiation. The two flow velocities acting on a movable bed particle are obtained by interpolating the velocities of nearby inner fluid particles to this reference particle using the SPH kernel function, as follows (Ran et al., 2013):

$$u_{bottom} = \frac{\sum_b m_b W(r_{ab}, h)(u_b \cos\theta - v_b \sin\theta)}{(\rho_a + \rho_b)/2} \tag{21}$$

$$v_{bottom} = \frac{\sum_b m_b W(r_{ab}, h)(u_b \sin\theta + v_b \cos\theta)}{(\rho_a + \rho_b)/2} \tag{22}$$

where θ = slope angle of the plane on the interface particle on the bed, which is the averaged slope of the neighbouring bottom particles within three times of the kernel range; and u_b and v_b = horizontal and vertical velocities of the neighbouring inner fluid particles. The summation is carried out for the inner particles only and both velocity components should be decomposed and taken into account due to the slope angle.

If both of the velocities represented by Equations (21) and (22) exceed the critical pick-up value, which depends on the different sediment grain properties, the reference interface bed particle is regarded as being erodible. This criterion is mathematically defined by

$$u_{bottom} > u_{cr} \tag{23}$$

$$v_{bottom}(t + \Delta t) - v_{bottom}(t) > v_{cr} \tag{24}$$

where u_{cr} and v_{cr} = threshold pick-up velocities of the sediment particle. Since the real sediment pick-up process is mainly related to the flow shear stress acting in the horizontal direction and the near-bed turbulent fluctuation which acts in the vertical direction, we hereby use the horizontal velocity combined with the variations of vertical velocity to judge the critical scouring process.

As for the evaluations of u_{cr} and v_{cr}, the following empirical formula can be used

$$u_{cr} = 1.2\sqrt{gD}\log_{10}\frac{14.7h}{D^{0.75}} \tag{25}$$

$$v_{cr} = F_{collision}\Delta t / m \tag{26}$$

Equation (25) is based on the B. C. Кнороз's formulation (Qian, 2003), in which D = sediment mean diameter and h = flow depth. Equation (26) follows Hayashi et al. (2003), in which $F_{collision}$ = fluid force on the bed surface and is assumed to be the self-weight of

sediment grain under critical condition, m = mass of sediment grain and Δt = computational time step.

Free Surfaces and Fixed Solid Boundaries

Free Surfaces

More detailed free surface treatment was presented by Shao and Lo (2003). Here only a brief summary is provided. If the density of a particle is 10% below the reference density, it can be judged as the surface particle. Then a zero pressure is imposed as the known boundary condition. The majority of the free surface particles can be found in this way and some misjudgements can happen, but this has no much influence on the computational accuracy.

Impermeable/Fixed Solid Walls

The impermeable/fixed solid walls are modelled by the particles that are fixed along the boundary lines. In ISPH algorithm, the PPE is solved on these wall particles with the imposition of a zero pressure gradient condition between the dummy and the wall particles. As the fixed dummy particles are used, an equivalence of non-slip boundary condition is enforced. However, different slip boundary conditions can also be easily implemented by using the mirroring particle technique as originated by Cummins and Rudman (1999). These impermeable/fixed solid wall particles are not erodible, which are different from the interface bed particles as shown in Fig. 1.

Model Application I – Dam Break Flow of Spinewine (2005)

Domain Setting and Computational Parameters

To validate the proposed ISPH erosion model, in this section it is applied to the benchmark test of dam break flow over a movable sediment bed. The laboratory experiment was carried out by Spinewine (2005). The computational domain includes a water tank separated by an instantaneously removed gate from the downstream side, and the tank bottom is covered by a layer of movable sediment materials. This case has also been numerically investigated by Shakibaeinia and Jin (2011) using the MPS method coupled with a multi-phase rheological model. We will use both the experimental and numerical data to validate the ISPH erosion model by comparing the free surface and bed evolution profiles.

The setup of numerical tank is shown in Fig. 2. The water column is 3 m wide and 0.35 m high, consistent with the experimental (Spinewine, 2005) and numerical (Shakibaeinia and Jin, 2011) settings. A particle spacing ΔX = 0.01 m is used for both the water and the sediment materials. The thickness of the sediment bed layer is arranged to be thick enough to ensure full development of the scour hole during the simulation time. According to Shakibaeinia and Jin (2011), the sediment sample has a limited size, but for simplicity we regard the sediment medium as being continuous and thus we can use the same particle resolution as that in the water region. At the beginning of computation, all of the particles are arranged on a uniform square grid system. Different from the multi-phase MPS simulations of Shakibaeinia and Jin (2011), in this study we do not consider the rheological behaviours of the sediment flow. Our main focus is to validate the sediment erosion model based on the principle of pick-up flow velocity.

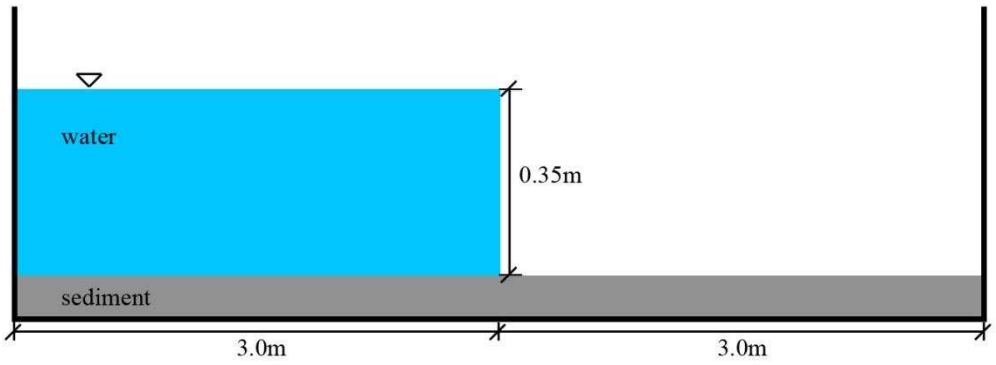

Fig. 2 Schematic setup of movable bed dam break flow (Spinewine, 2005)

Model Validations and Result Analysis

To validate the model, the computed free surfaces and bed evolution profiles by the ISPH scour model are compared with the experimental data (Spinewine, 2005) and MPS results (Shakibaeinia and Jin, 2011) in Figs. 3 and 4 at three different time instants after the dam break, i.e. t = 0.25 s, 0.5 s and 0.75 s, respectively.

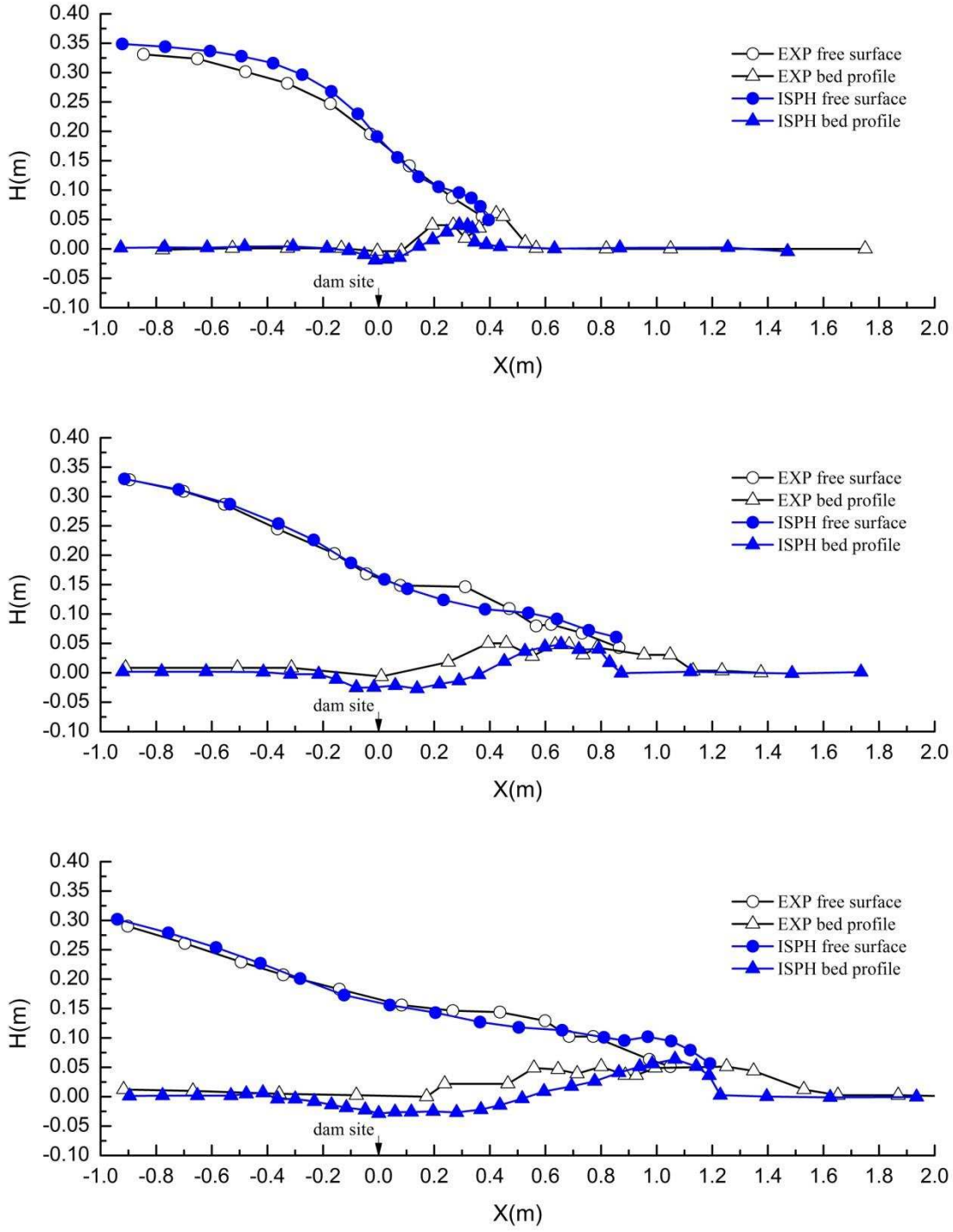

Fig. 3 Comparisons of free surface and bed evolution profiles between ISPH simulations and experimental data (Spinewine, 2005) at t = 0.25 s, 0.5 s and 0.75 s (from up to down)

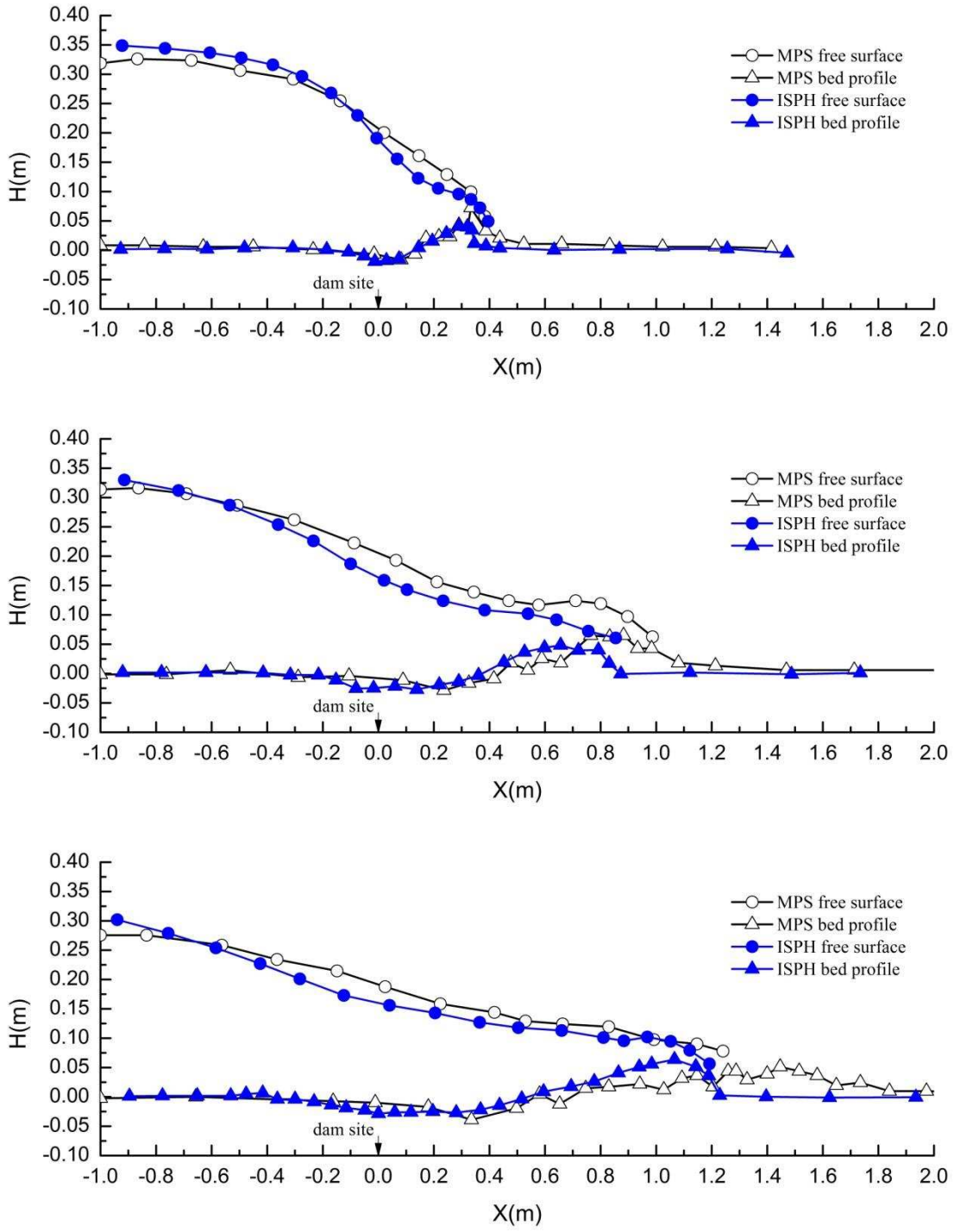

Fig. 4 Comparisons of free surface and bed evolution profiles between ISPH simulations and MPS results (Shakibaeinia and Jin, 2011) at t = 0.25 s, 0.5 s and 0.75 s (from up to down)

The comparisons in Fig. 3 indicated that the ISPH computed free surface profiles matched the experimental data of Spinewine (2005) quite well for the first two time instants. However, relatively large errors appeared near the free surface leading edge at time $t = 0.75$ s and the ISPH model over-predicted the flow propagation. As for the sediment bed profiles, the ISPH model well predicted the maximum sediment layer height, but there exist some discrepancies in the bed evolution profile and the ISPH seemed to under-predict the sediment bed movement. From Fig. 4, it is noted that the ISPH computed sediment scour profiles matched the multi-phase MPS computations of Shakibaeinia and Jin (2011) in a quite satisfactory manner, although different sediment initiation modes were used in the two models. In Shakibaeinia and Jin (2011), they employed a multi-phase formulation by considering the non-Newtonian behaviour of the fluids, while in the present ISPH erosion model only a simple eddy viscosity correction model represented by Equation (20) is used. The maximum scour depth seems to occur at the early stage of the dam break flow and then elongate afterwards. Although the ISPH computations matched the MPS scour profiles near dam site well, there are obvious discrepancies in the downstream bed evolutions, which explained the disagreement between the two numerical water surface profiles.

In engineering practice, it is more common to study the macro flow and sediment features, such as the water leading edge, maximum scour depth and bed height. To provide useful information on these and also quantify the simulation errors, the ISPH computed representative parameters at three time instants ($t = 0.25$ s, 0.5 s and 0.75 s) are compared with the experimental data and MPS results in Table 1. It shows that both numerical models can reasonably predict the experimental observations. Generally speaking, MPS seemed to better predict the early stage of the dam break flow while SPH better predict the later stage.

Table 1 ISPH computed water leading edge, maximum scour depth and bed height, compared with experimental data and MPS results

Key parameters (t = 0.25 s)	Results (m)		
	ISPH	MPS	EXP
Water leading edge	0.391	0.383	0.374
Maximum scour depth	0.027	0.016	0.007
Maximum bed height	0.045	0.072	0.059

Key parameters (t = 0.50 s)	Results (m)		
	ISPH	MPS	EXP
Water leading edge	0.867	0.987	0.868
Maximum scour depth	0.027	0.028	0.007
Maximum bed height	0.056	0.065	0.049

Key parameters (t = 0.75 s)	Results (m)		
	ISPH	MPS	EXP
Water leading edge	1.157	1.241	1.049
Maximum scour depth	0.027	0.039	0.000
Maximum bed height	0.068	0.051	0.048

Furthermore, to demonstrate the sensitivity of numerical results on the particle spacing and evaluate the convergence of the model, three different particle sizes of ΔX = 0.02 m, 0.01 m and 0.005 m were used and the error norms between the ISPH and experimental free surfaces (Spinewine, 2005) are shown in Table 2, also for the three time instants. The comparisons in Table 2 have demonstrated that the error norms consistently decrease as the spatial resolutions increase, i.e. when the particle sizes become smaller. As a result, more refined ISPH simulations can provide better agreement with the experimental data, indicating the convergence of the model.

Table 2 Error norms between ISPH and experimental free surfaces for ΔX = 0.02 m, 0.01 m and 0.005 m

Time t (s)	Error norms		
	ΔX = 0.02 m	ΔX = 0.01 m	ΔX = 0.005 m
0.25	0.102	0.069	0.065
0.50	0.098	0.088	0.083
0.75	0.122	0.109	0.091

Discussions on Dam Break Flow Features

To study the spatial and temporal flow features of the dam break flow over a movable bed, the ISPH computed particle snapshots and velocity fields are shown in Figs. 5 and 6 at time t = 0.25 s, 0.5 s and 0.75 s, respectively, after the dam is broken. It is shown from Fig. 5 that at the early stage of the dam break (t = 0.25 s), the water wave propagated on the movable bed and scoured the bed materials, thus the scour hole developed very fast. At the later stage of the dam break flow (t = 0.75 s), in comparison, as the flow velocity deceased, the development of the hole erosion also decreased gradually. This is demonstrated by the fact that the scour hole tended to be flattened along the downstream direction, while its vertical development has slowed down. In the ISPH simulations, there exists a distinct scouring region near the original dam site. The computed flow features are similar to those observed in the experiment of Spinewine (2005) and numerical MPS simulations of Shakibaeinia and Jin (2011).

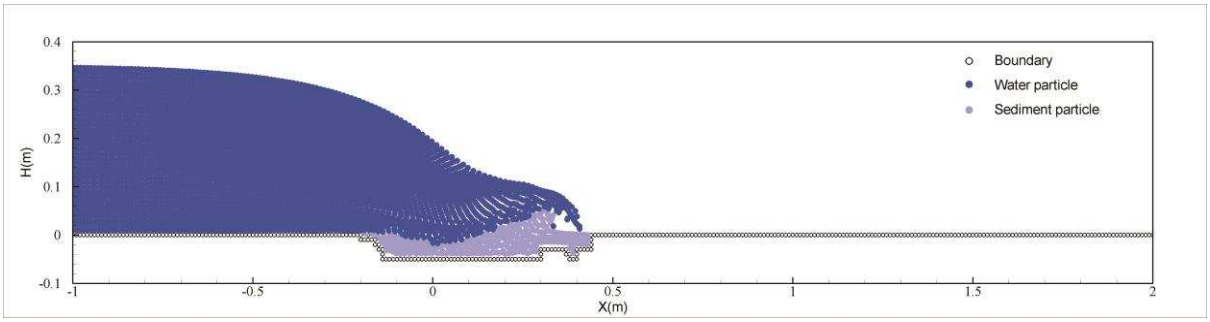

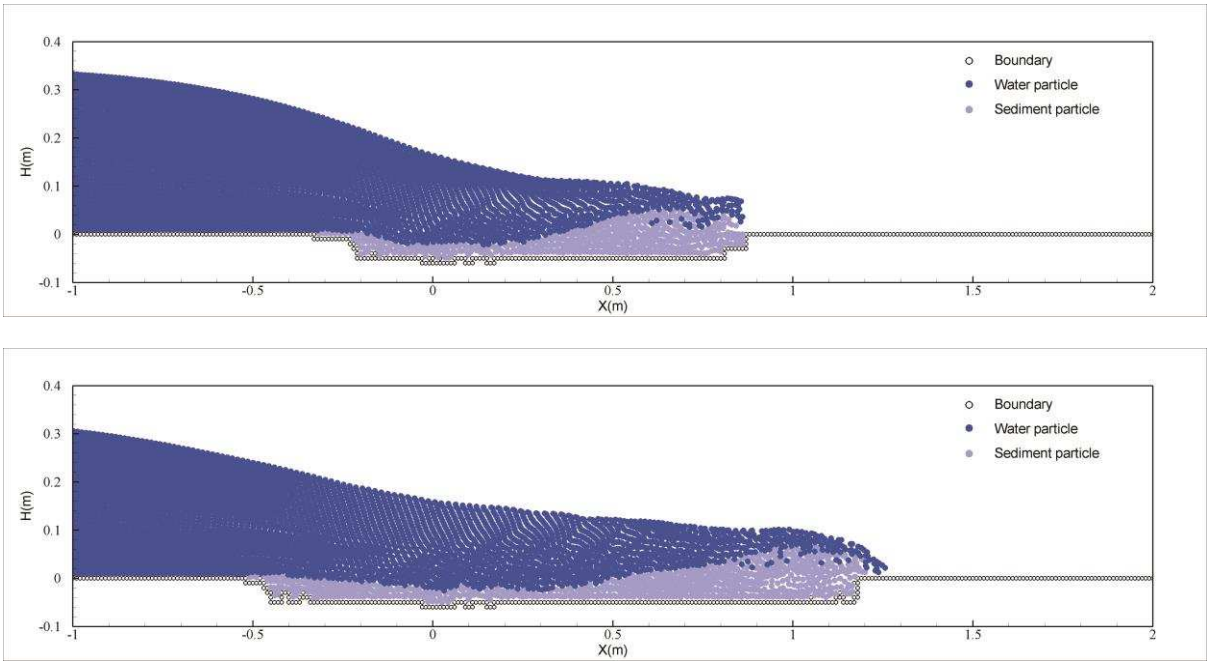

Fig. 5 ISPH computed particle snapshots of dam break flow over a movable sediment bed at time t = 0.25 s, 0.5 s and 0.75 s (from up to down) after the dam break

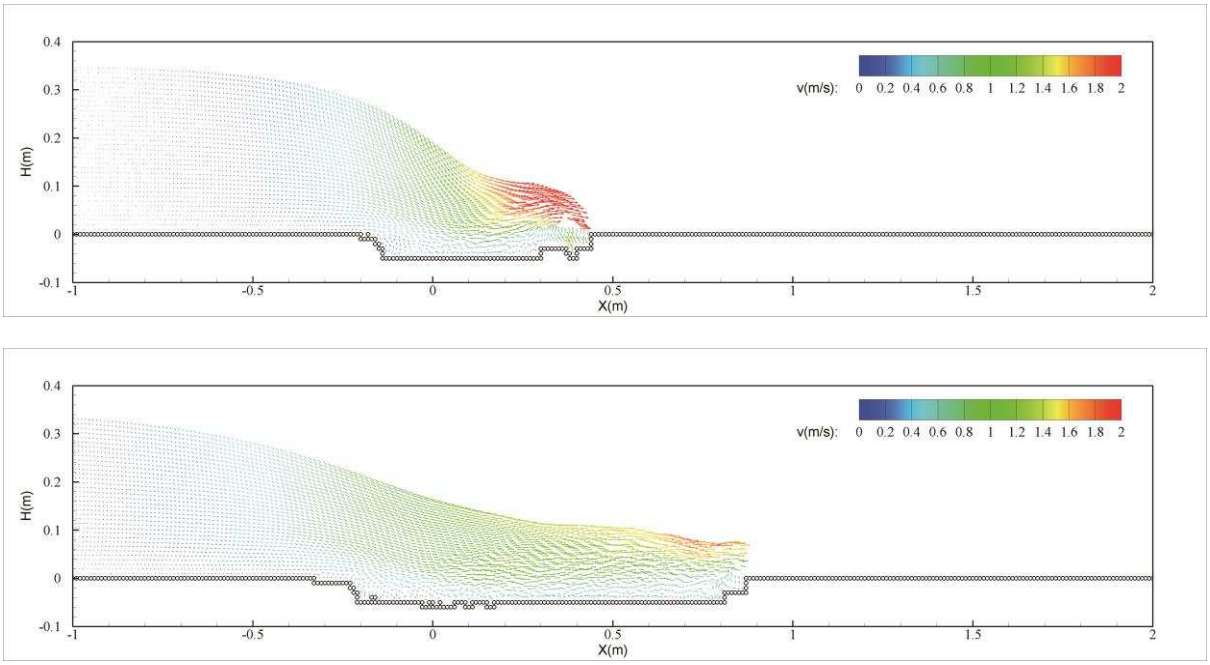

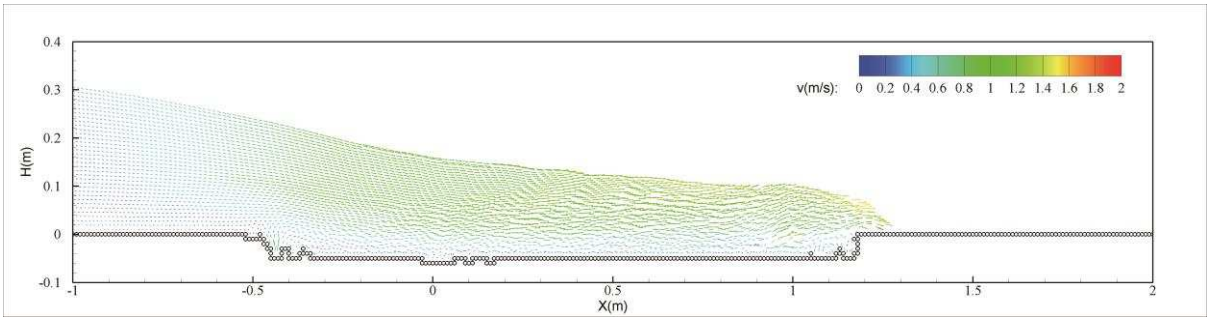

Fig. 6 ISPH computed velocity fields of dam break flow over a movable sediment bed at time t = 0.25 s, 0.5 s and 0.75 s (from up to down) after the dam break

The computed flow velocity fields in Fig. 6 indicated that the dam break flow over a movable bed is much milder as compared with the dam break flow over a fixed rigid bed. This is due to that the scouring process reduced the flow intensity and dampened the flow energy. Thus much smaller scale of the velocity distribution patterns has been observed. The existence of scour hole increased the flow area and thus reduced the flow velocity. It is shown that the flow propagations resembled like a typical bore flow with the larger velocities appearing near the leading front. It can also be observed that the vertical velocity and its variation are large near the bed during the early stage of the scouring, thus the scour hole developed very fast. As time went on to the later stage of the flow, the vertical velocity differences became small near the scour hole and the development of the scouring depth tended to be stable.

Two-phase Water-Sediment Interactions

To demonstrate the interactions between the water and sediment phases during the scouring and bed movement, the computed two-phase velocity and pressure fields near the water-sediment interface are shown in Fig. 7 (a) and (b), respectively, at selected time t = 0.25 s after the dam break.

The two-phase velocity fields in Fig. 7 (a) show that although the velocity is continuous across the water-sediment interface, the overall velocity in the water region is much larger than that within the sediment area. Thus there exists a drag effect in the longitudinal direction for the sediment moving forward. Besides, the dam break flow also generated sufficient turbulence near the bed and the turbulence suspended the sediment particles in an upward direction, which is particularly true under the leading front of the flow. Within the sediment layer, the velocity decreased towards the lower bed and the sediment motion near the dam site nearly settled down. Examining the pressure fields in Fig. 7 (b), we can see the advantage of the ISPH modelling approach to obtain relatively noise-free pressure pattern even across the water-sediment interface. Following Equation (19), there should be no pressure

discontinuities at the two-phase interface and this has well been achieved in the simulations. One distinct large pressure area appears near the front of the scour hole, indicating further potential erosions in this region.

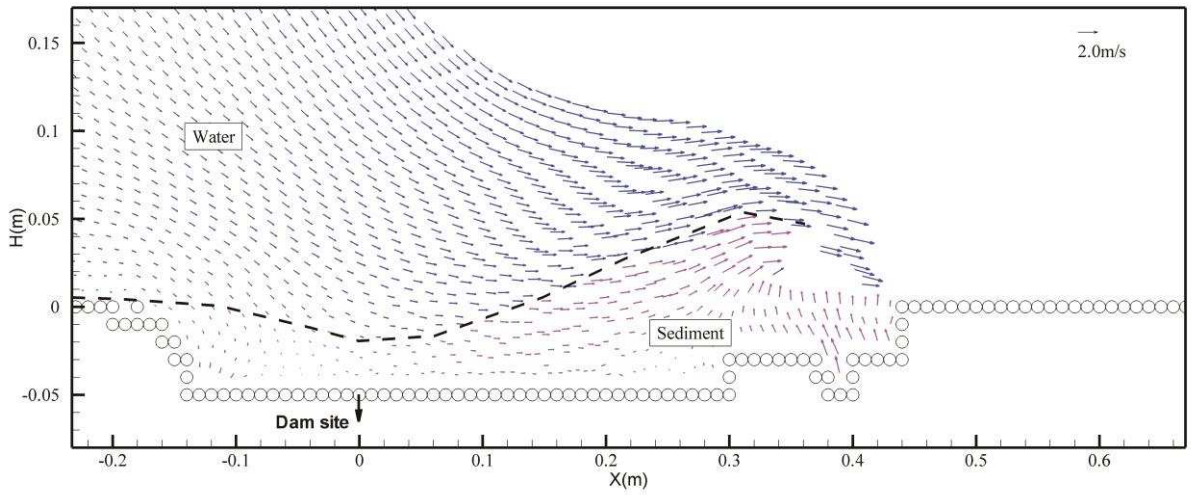

(a)

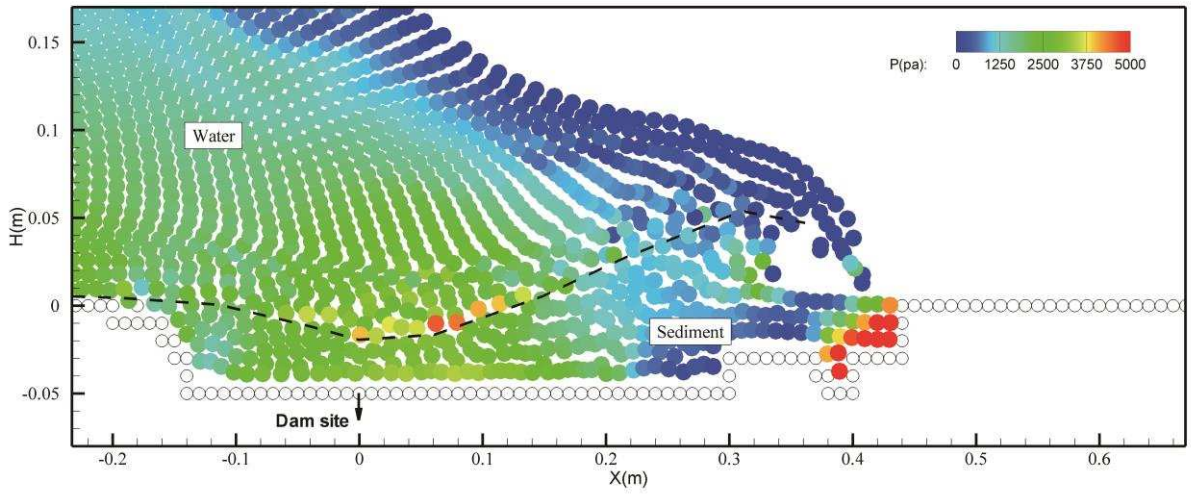

(b)

Fig. 7 Two-phase water-sediment interactions after the dam break (a) velocity field; and (b) pressure field

Vertical distribution profiles of velocity, concentration and stresses

In a latest benchmark work, Spinewine and Capart (2013) measured detailed flow and sediment information in a dam break flow over the movable bed and investigated the vertical distribution profiles of several key parameters. To further demonstrate the robustness of the proposed ISPH modelling technique, the computed longitudinal velocity, sediment concentration, and normal and tangential stresses at selected vertical locations of the dam break flow are shown in Figs. 8 and 9, respectively.

For the instantaneous velocity and concentration profiles at time t = 0.75 s in Fig. 8, we plotted them at two different vertical locations by following Spinewine and Capart (2013). One is located in the upstream region and another is near the flow front, defined as the free-water and surface-confined section by Spinewine and Capart (2013). The SPH computations of the velocity profile are quite consistent with the experimental and numerical findings of Spinewine and Capart (2013), in that the velocity variations in the free-water layer demonstrate an almost constant pattern while they decrease in a linear manner inside the movable bed load layer. As for the sediment concentration profile, it is zero on the surface for the free-water case but attains a non-zero value for the surface-confined case, and also it shows a linear increase within the bed load layer. However, some discrepancies appear near the lower interface between the movable sediment layer and underlying immobile bed. This is due to that in the experiment of Spinewine and Capart (2013), the sediment particles always mixed with the water so the concentration profile changed at the interface between the movable layer and immobile bed. In the SPH simulations, however, the sediment layer was initiated and moved without the mixed water inside and the concentration was calculated as the sediment particles vs. water particles, thus the concentration profile quickly approaches to the maxima within the movable layer.

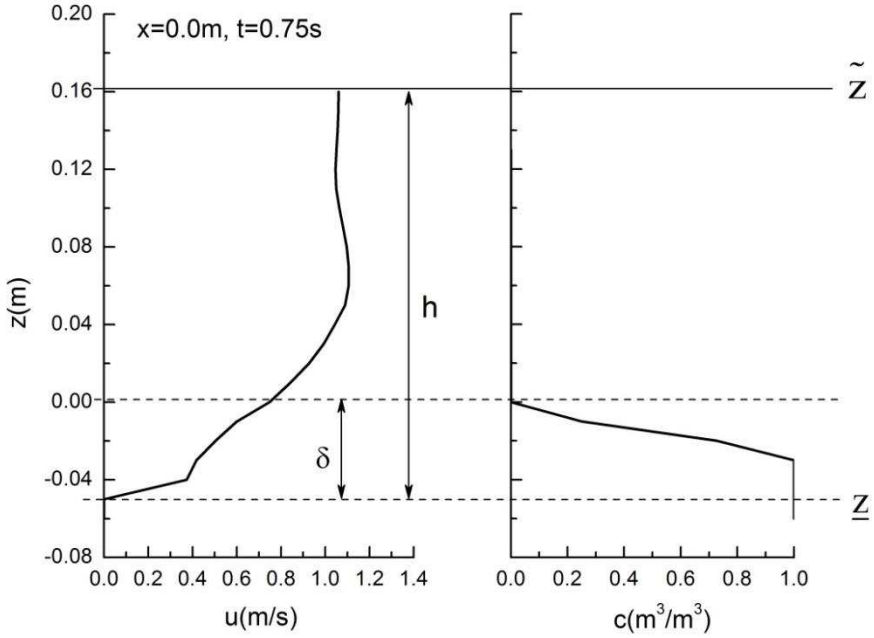

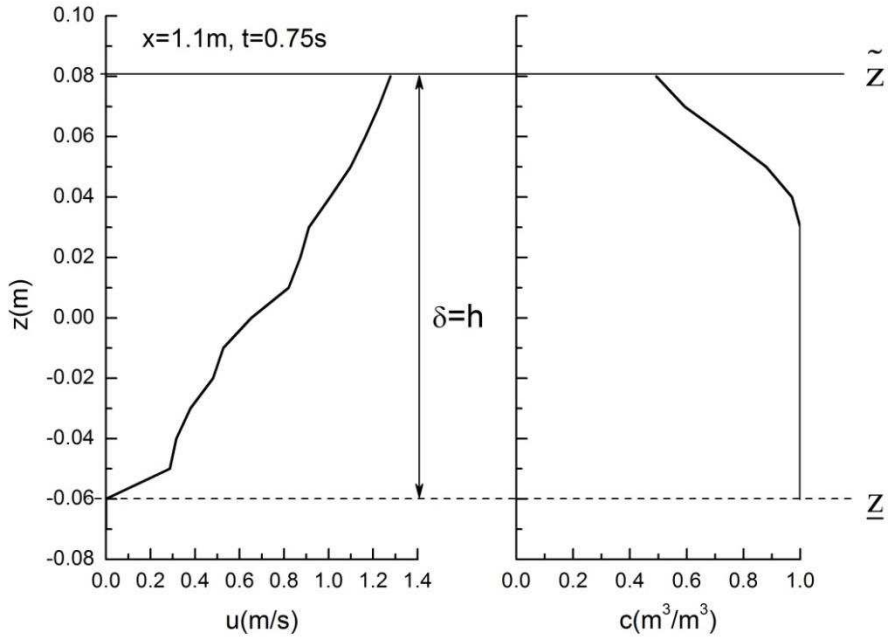

Fig. 8 Instantaneous velocity (left) and concentration (right) profiles at free-water (x = 0.0 m) and surface-confined (x = 1.1 m) locations, where δ is thickness of movable sediment layer and h is total flow depth confined between the free surface and immobile bed

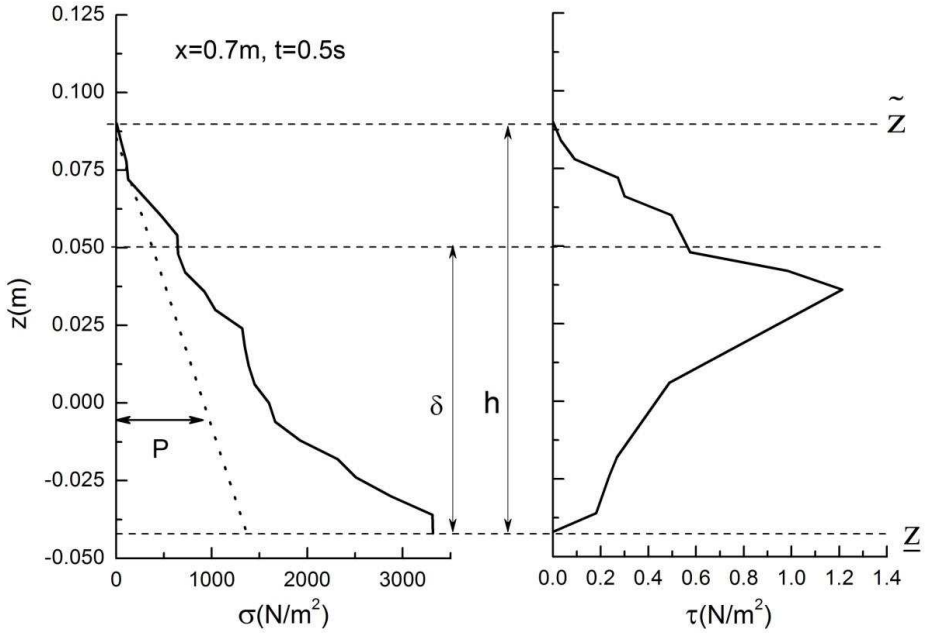

Fig. 9 Instantaneous normal (left) and tangential (right) stress profiles at free-water location (x = 0.7 m)

With regard to the normal and tangential stress profiles computed at time t = 0.5 s as shown in Fig. 9 for the location of the free-water zone, the SPH computed normal stress profile compares quite well with the numerical derivations of Spinewine and Capart (2013, in their Fig. 7), in that the normal stress follows a quasi-hydrostatic pattern in the water region but increases non-linearly inside the movable sediment layer. This generated sufficient thrust to initiate the sediment particles into the motion. On the other hand, the corresponding tangential stress distribution shows a zero value on the free surface, increases linearly towards the water-sediment interface and decreases to zero again on the immobile bed. It is interesting to note there is a shear stress jump immediately inside the bed load layer and the maximum value is found somewhere below the interface. This is the area where the sediment grains are mostly influenced by the fluid drag. Although there is no reference data available for a comparison, the tendency of the tangential stress curve seems to be reasonable. Also, we need to realize that the differences in the normal stress profile between Spinewine and Capart (2013) and present work are probably attributed to the fact that the former used the shallow water theory but the latter solved the full Navier-Stokes equations.

Here it needs to be mentioned that the above computed profiles of velocity, concentration and two components of the stresses demonstrate good similarity in other vertical sections as well, indicating the accuracy of numerical results and the repeatability of fundamental water-sediment flow mechanisms. The relevant analysis disclosed that for the movable bed dam break flows, the sediment concentration and influence are so substantial as to change the nature of the fluid properties. Besides, Ferrari et al. (2010) used a weakly compressible SPH (WCSPH) method to solve dam break flow over a rigid bed and the computed flood flow behaviours are different from those found in the present movable bed conditions, which is the result of the significant influences from the eroded and transported sediment phases.

Model Application II – Dam Break Flow of Capart et al. (2002)

To further validate the proposed ISPH erosion model and investigate the sensitivity of the threshold pick-up velocity in Equation (24), another test based on the work of Capart et al. (2002) is carried out in this section. The experimental conditions are summarized as follows. A horizontal flume of rectangular cross-section is used. The test reach had the length of 2.5 m, width of 10 cm and side-wall height of 35 cm. Following the sudden raise of a narrow gate retaining an upstream reservoir of still water, an idealised dam-break wave was released over an erodible bed. A sediment layer of constant thickness of approximately 5 to 6 cm extends both upstream and downstream of the dam. The still reservoir flow depth is 10 cm above the top of the sediment bed. The sediment has a mean diameter of 3.5 mm and relative density of 1.54. In the ISPH simulations, a particle size of ΔX = 5.0 mm is used. The setup sketch of the numerical flume is shown in Fig. 10.

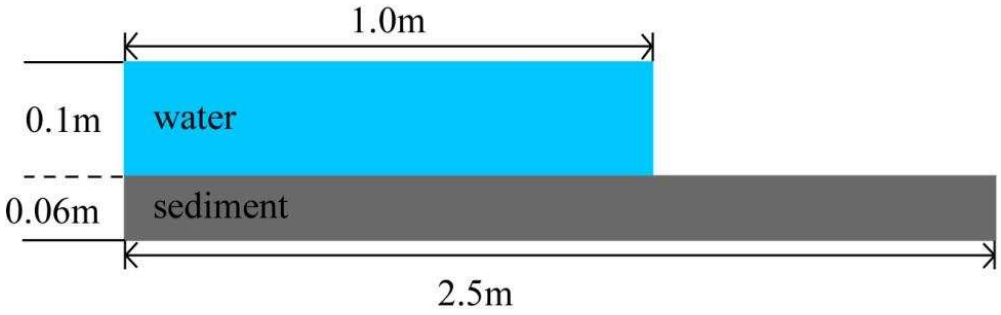

Fig. 10 Setup of numerical flume for movable bed dam break flow (Capart et al., 2002)

Following the numerical simulations, the ISPH computed free surface and bed evolution profiles at time t = 0.75 s after the dam break are shown in Fig. 11, and compared with the experimental data of Fraccarollo and Capart (2002). Meanwhile, to investigate the sensitivity of the critical pick-up velocity in the vertical direction, V_{cr} in Equation (24), two additional tests were made by using a value of $5V_{cr}$ and $V_{cr}/5$, respectively. The results are also shown in the same figure. On the one hand, it shows that the ISPH simulations can well reproduce the experimental free surfaces and bed evolutions including both the upper and lower bedload profiles. On the other hand, it has demonstrated the sensitivity of the threshold pick-up velocity on the sediment movement features: Increasing the pick-up velocity by 5 times did not much influence the free surfaces but more on the sediment bed profiles, while decreasing the pick-up velocity by 5 times made almost no difference in the overall predictions. As the pick-up velocity is related to the flow turbulence, this implies that the sediment suspension is more influential on the bed evolutions rather than the water surface developments. In addition, it should be mentioned here that there are two bed profiles in each subfigure in Fig. 11 and they correspond to the upper and lower limit of the movable bed, defined as the moving sediment and immobile granular substrate by Capart et al. (2002).

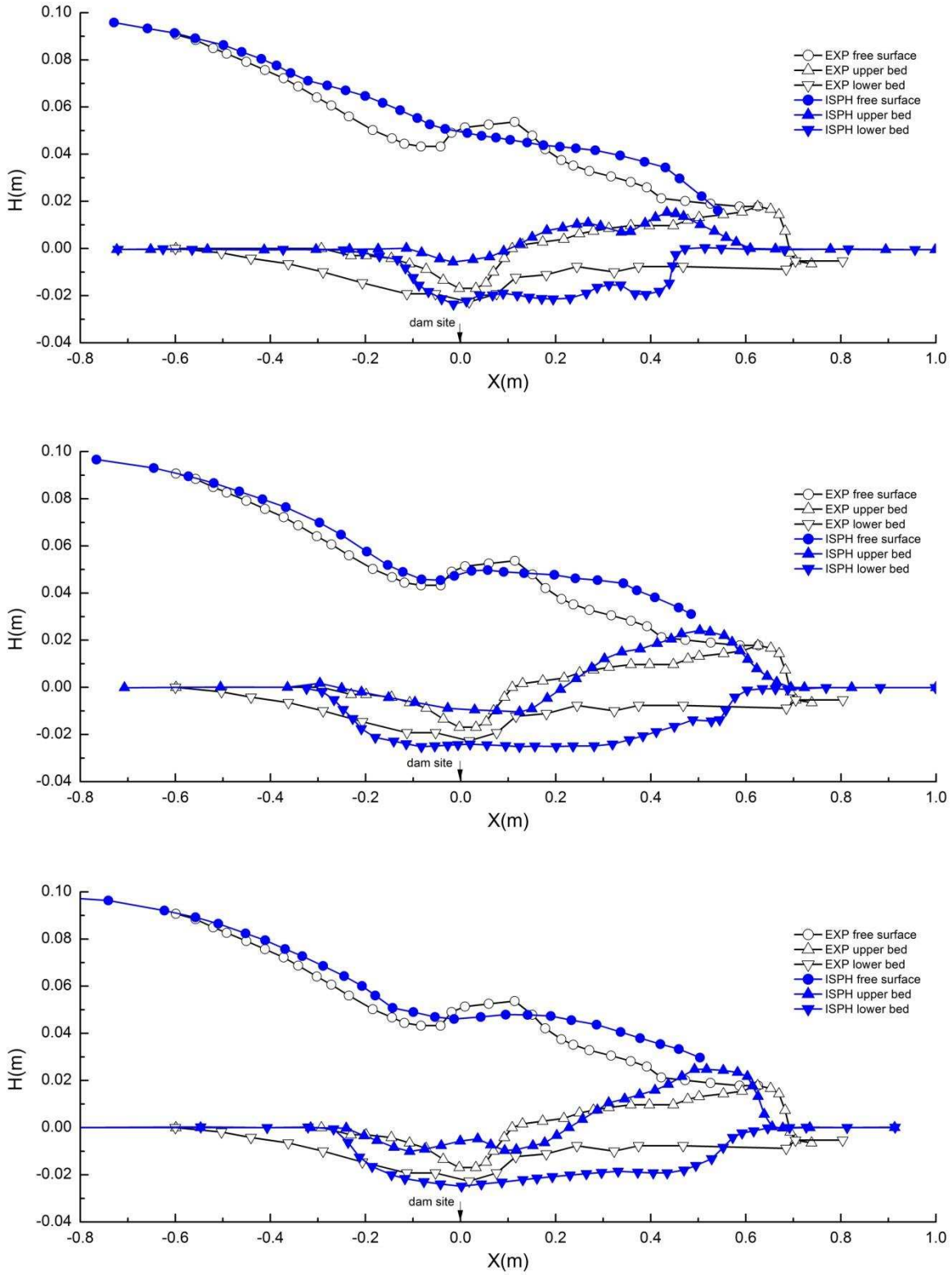

Fig. 11 Comparisons of free surface and bed evolution profiles between ISPH simulations and experimental data (Fraccarollo and Capart, 2002) at t = 0.75 s for threshold pick-up velocity of $5V_{cr}$, V_{cr} and $V_{cr}/5$ (from up to down)

Finally, to make further investigations into the influence of critical pick-up velocity V_{cr} on the dam break flows, the time-dependent leading edges of the water surface and sediment bed profile are shown in Fig. 12 (a) and (b), respectively, for the three different pick-up velocities as used before. The computed results are also compared with the experimental data of Fraccarollo and Capart (2002). It is shown that by decreasing the critical pick-up velocity the numerical simulations are globally closer to the experiment. However, further decrease of the pick-up velocity showed little improvement since the results tended to stabilize. In Fig. 12 (a), for the leading edge of the water surface, a larger critical pick-up velocity matched the experiment better at the beginning of the dam break while a smaller one matched the experiment more favourably at the later stage. On the other hand, in Fig. 12 (b) for the leading edge of the sediment bed profile, the choice of different pick-up velocities only affected the numerical accuracy at the early stage of the simulation, but the differences became much smaller with the elapse of the time. Generally speaking, more sound sediment initiation mechanisms should be included to improve the modelling accuracy in future studies.

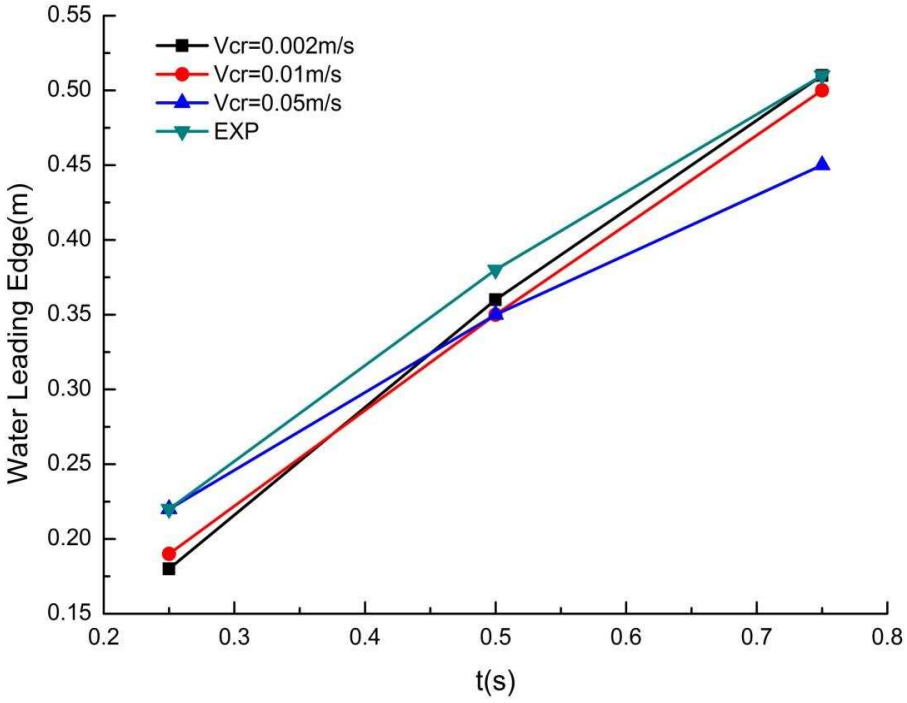

(a)

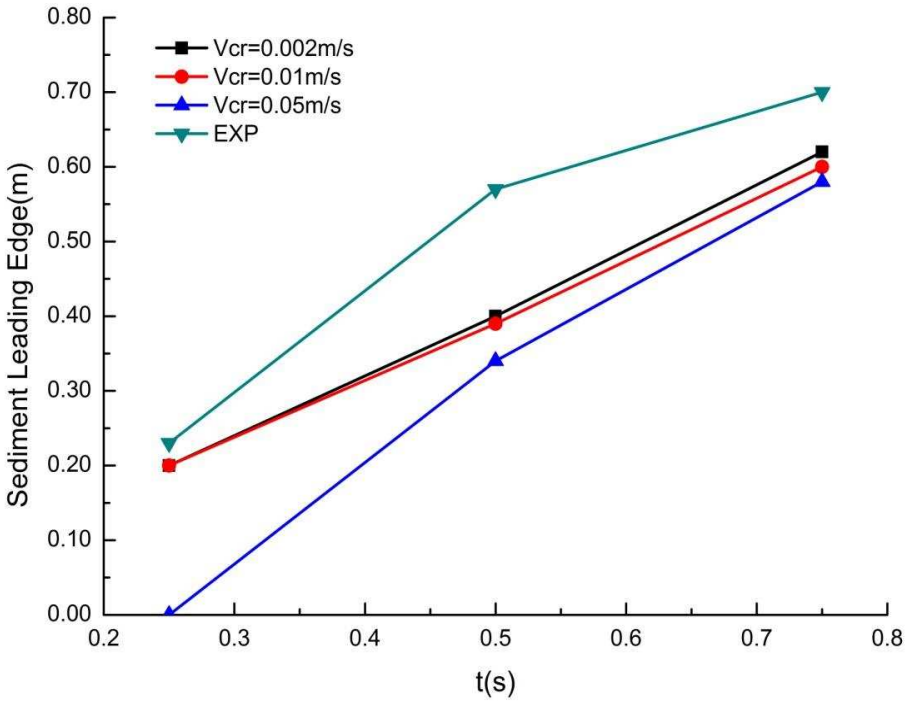

(b)

Fig. 12 Time-dependent leading edge for different pick-up velocities (a) leading edge of water surface; and (b) leading edge of sediment profile

Conclusions

An ISPH erosion model based on the pick-up flow velocity has been developed to simulate the dam break flows over a movable sediment bed. The computed results are in good agreement with either the experimental or other numerical data. The ISPH computations have realistically disclosed the spatial and temporal evolution features of the free water surface, sediment bed scour and bedload movement. It is found that the bed scour started near the original dam site and propagated towards the downstream direction with a decreasing trend in the vertical scour depth. An alternative ISPH computation using three different particle spacing verified the convergence of the numerical scheme. Sensitivity analysis on the critical pick-up velocity has also been carried out to demonstrate the importance of turbulence and velocity fluctuations near the bed on sediment scouring process. The two-phase velocity and pressure fields computed near the interface and the vertical distribution profiles of the

velocity, concentration and two components of the stresses have disclosed complex water-sediment interactions during the sediment grain initiation and follow-on movement.

Future work would be needed to improve the model capacity by addressing different sediment initiation mechanisms, such as the critical shear stress. Besides, the rheological properties of the sediment-laden flow should also be considered, which will be more useful in the hyper-concentrated flow applications in a practical field.

Acknowledgements

We kindly acknowledge the support of the Research Fund of the Ministry of Water Resources of China (No. 201201041-02) and the Major State Basic Research Development Program (973 program) of China (No. 2013CB036402).

References

Capart, H., Young, D. L. and Zech, Y. (2002), Voronoï imaging methods for the measurement of granular flows, Experiments in Fluids, 32, 121-135.

Cummins, S. J. and Rudman, M. (1999), An SPH projection method, Journal of Computational Physics, 152, 584–607.

Ferrari, A., Fraccarollo, L., Dumbser, M., Toro, E. F. and Armanini, A. (2010), Three-dimensional flow evolution after a dam break, Journal of Fluid Mechanics, 663, 456–477.

Fraccarollo, L. and Capart, H. (2002), Riemann wave description of erosional dam-break flows, Journal of Fluid Mechanics, 461, 183-228.

Gotoh, H., Shibahara, T. and Sakai, T. (2001), Sub-particle-scale turbulence model for the MPS method – Lagrangian flow model for hydraulic engineering, Comp. Fluid Dyn. J., 9, 339-347.

Gotoh, H. and Sakai, T. (2006), Key issues in the particle method for computation of wave breaking, Coast. Engng., 53, 171–179.

Hayashi, M., Gotoh, H., Sakai, T. and Ikari, H. (2003), Lagrangian gridless model of toe scouring of seawall due to tsunami return flow, Proceedings of Asia and Pacific Coast, APAC 2003.

Hu, X. Y. and Adams, N. A. (2007), An incompressible multi-phase SPH method, Journal of Computational Physics, 227(1), 264-278.

Ikari, H., Gotoh, H. and Arai, T. (2010), Fluid-elastoplastic hybrid model for computational mechanics of wave-induced sea cliff erosion, Proceedings of Coastal Engineering, Japan Society of Civil Engineers, 66(1), 916-920 (in Japanese).

Janosi, I. M., Jan, D., Szabo, K. G. and Tel, T. (2004), Turbulent drag reduction in dam break flows, Experiments in Fluids, 37, 219–229.

Lauber, G. and Hager, W. H. (1998), Experiments to dam break wave: horizontal channel, Journal of Hydraulic Research, 36(3), 291-307.

Lind, S. J., Xu, R., Stansby, P. K. and Rogers, B. D. (2012), Incompressible smoothed particle hydrodynamics for free-surface flows: A generalised diffusion-based algorithm for stability and validations for impulsive flows and propagating waves, Journal of Computational Physics, 231(4), 1499-1523.

Manenti, S., Sibilla, S., Gallati, M., Agate, G. and Guandalini, R. (2012), SPH simulation of sediment flushing induced by a rapid water flow, Journal of Hydraulic Engineering, ASCE, 138(3), 272-284.

Monaghan, J. J. (1992), Smoothed particle hydrodynamics, Annual Review of Astronomy and Astrophysics, 30(1), 543–572.

Qian, N. (2003), Sediment Mechanics, Beijing Scientific Publication (in Chinese).

Ran, Q., Tong, J., Fu, X., Liao, Q. and Shao, S. (2013), Incompressible SPH simulations of bed scour under dam break flow, Proceedings of 2013 IAHR World Congress, A10998, Chengdu, China, Sep 8-13.

Shakibaeinia, A. and Jin, Y. C. (2011), A mesh-free particle model for simulation of mobile-bed dam break, Advances in Water Resources, 34, 794–807.

Shao, S. D. and Lo, E. Y. M. (2003), Incompressible SPH method for simulating Newtonian and non-Newtonian flows with a free surface, Advances in Water Resources, 26, 787–800.

Shao, S. D. (2012), Incompressible smoothed particle hydrodynamics simulation of multifluid flows, Int. J. Numer. Meth. Fluids, 69, 1715–1735.

Sibilla, S. (2008), A SPH-based method to simulate local scouring, Proceedings of 19th IASTED International Conference - Modeling and Simulation, manuscript No. 620-096, 9-14.

Spinewine, B. (2005), Two-layer Flow Behaviour and the Effects of Granular Dilatancy in Dam Break Induced Sheet-flow, PhD thesis, Univerisité de Louvain.

Spinewine, B. and Carpart, H. (2013), Intense bed-load due to a sudden dam-break, Journal of Fluid Mechanics, 731, 579-614.

Ulrich, C., Leonardi, M. and Rung, T. (2013), Multi-physics SPH simulation of complex marine-engineering hydrodynamic problems, Ocean Engineering, 64, 109–121.

Xia, J., Lin, B., Falconer, R. and Wang, G. (2010), Modelling dam-break flows over mobile beds using a 2D coupled approach, Advances in Water Resources, 33, 171–183.

Xu, R., Stansby, P. and Laurence, D. (2009), Accuracy and stability in incompressible SPH (ISPH) based on the projection method and a new approach, J. Comput. Phys., 228, 6703-6725.

Zhang, S. and Duan, J. G. (2011), 1D finite volume model of unsteady flow over mobile bed, Journal of Hydrology, 405, 57–68.